DOI: 10.1111/cgf.14673
Pacific Graphics 2022
N. Umetani, E. Vouga, and C. Wojtan
(Guest Editors)

*Volume 41 (2022), Number 7*

# Specular Manifold Bisection Sampling for Caustics Rendering

Jia-Wun Jhang and Chun-Fa Chang †

National Taiwan Normal University, Taiwan

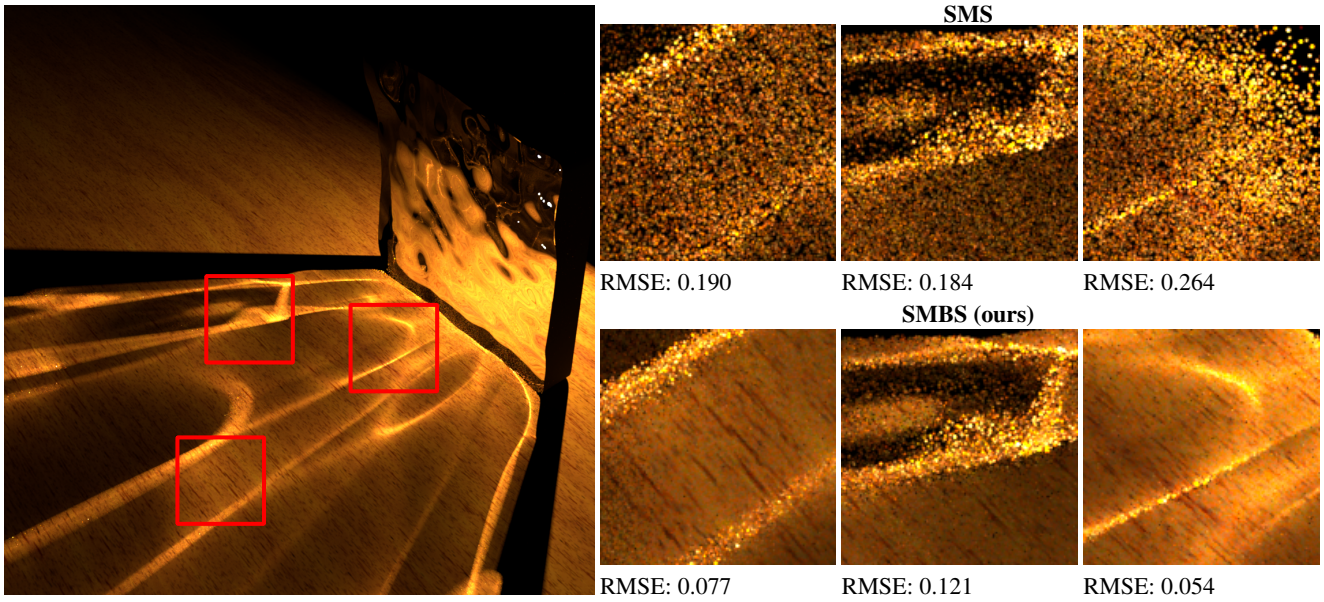


**Figure 1:** *Equal time comparison between SMS and our SMBS with the glass scene that showcases the caustics effect on the ground. Our approach has lower root mean square error (RMSE) than SMS.*

**Abstract**

*We propose Specular Manifold Bisection Sampling (SMBS), an improved version of Specular Manifold Sampling (SMS) [ZGJ20]. SMBS is inspired by the small and large mutations in Metropolis Light Transport (MLT) [VG97]. While the Jacobian Matrix of the original SMS method performs well in local convergence (the small mutation), it might fail to find a valid manifold path when the ray deviates too much from the light or bounces from a complex surface. Our proposed SMBS method adds a large mutation step to avoid such a problematic convergence to the local minimum. The results show SMBS can find valid manifold paths in fewer iterations and also find more valid manifold paths. In scenes with complex reflective or refractive surfaces, our method achieves nearly twice or more improvement when measured in manifold walk success rate (SR) and root mean square error (RMSE).*

**CCS Concepts**

• ***Computing methodologies*** → ***Rendering;***

## 1. Introduction

Path Tracing covers all paths in the Rendering Equation [Kaj86] theoretically, but not every path can be easily found in practice, such as the well-studied specular-diffuse-specular (SDS) paths. Recently Manifold Exploration [JM12] and Manifold Next-Event Es-

† Corresponding author

timation (MNEE) [HDF15] explore the surface manifold on refracted paths to connect to the light successfully.

Specular Manifold Sampling (SMS) [ZGJ20] improves MNEE further by sampling reflective objects to find more valid paths than MNEE. While the Jacobian Matrix of the SMS method performs well in local convergence, it might fail to find a valid manifold path when the ray deviates too much from the light or bounces from a complex surface. We propose Specular Manifold Bisection Sampling (SMBS) which adds a large mutation step to avoid such a problematic convergence to local minimum. The results show SMBS can find valid manifold paths in fewer iterations and also find more valid manifold paths than the original SMS.

## 2. Prior Work

Light Transport Simulation has been an important topic in computer graphics for many years. The original Ray Tracing [Whi80] simulates paths with reflection and refraction. The advent of the Rendering Equation [Kaj86] led to the popularity of Path Tracing, a Monte Carlo integration technique that simulates all possible light paths through random walk.

While Path Tracing simulates all possible paths to get a realistic picture, the random walk from the eye could miss the light to form a valid path, leading to long convergence time to form a noise-free picture. In contrast, Direct Lighting [SWZ96] and Bi-Directional Path Tracing (BDPT) [LW93] can efficiently find a valid path by forcibly connecting to the light.

BDPT generates eye paths and light paths by random walk before connecting to the light points, so it is still difficult to find the paths that pass through a small gap, such as the scenes where the light is behind an ajar door. In addition, the specular-diffuse-specular path is also difficult to be found through forcible connection because of the material constraint. Metropolis Light Transport (MLT) [VG97] [KSK01] first finds enough valid paths through BDPT, and then reuses these paths by mutation (disturbance) to quickly find many different valid paths.

Our work focuses on caustics rendering within the path tracing framework. The classic Photon Mapping [Jen96] offers a fast yet biased rendering method for caustics. The Vertex Connection and Merging (VCM) [GKDS12] offers a caustics rendering method by combining the Bidirectional Path Tracing and Photon Mapping with multiple importance sampling. Recently Manifold Exploration [JM12], Manifold Next Event Estimation (MNEE) [HDF15], and Specular Manifold Sampling (SMS) [ZGJ20] were proposed to quickly find the valid caustics paths. We will discuss them in more detail in Section 3.

## 3. Background

The caustics effects in the scene are caused by refractive or reflective surfaces. Take Figure 2 as an example. The caustics appear on $x_1$ when the light from $x_4'$ is refracted by the transparent sphere. However when we perform path tracing, the initial path starting from $x_1$ might find $x_2, x_3, x_4$ and miss the light at $x_4'$. Manifold Exploration [JM12] offers a solution. The first step generates $x_1, \ldots, x_4$ by random walk. Although it has not found the light at $x_4'$ initially,

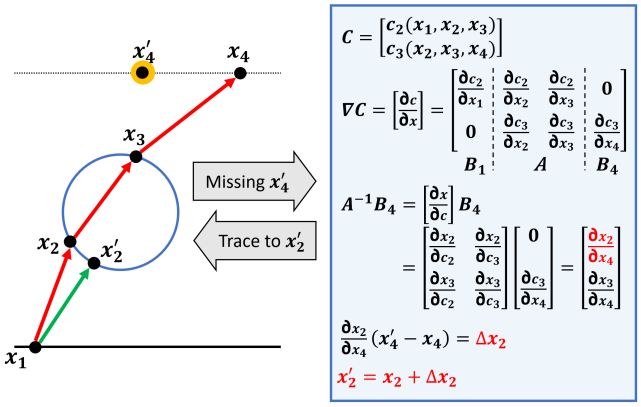


**Figure 2:** *The calculation process of Manifold Exploration.*

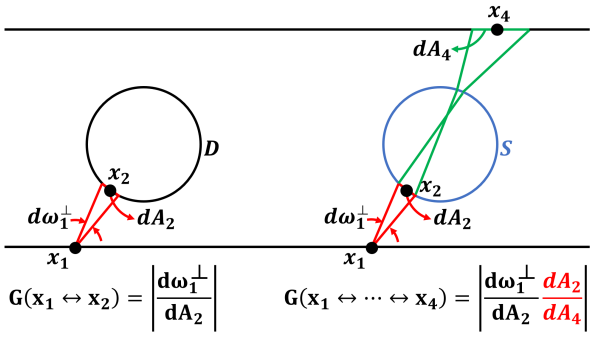


**Figure 3:** *The geometry factor (left) and the generalized geometry factor (right).*

the main purpose of this step is to get all the manifold points of reflection and refraction on the path. The second step uses the curvature constraint of each point (e.g., $c_2$ and $c_3$) to build a constraint matrix C, which then yields the Jacobian matrix $\bigtriangledown C$. This allows us to move toward the light $x_4'$ by $A^{-1} \cdot B_4 \cdot \Delta x_4$ to find the desired $x_2$. Repeat steps one and two until the ray hits the light. Algorithm 1 shows the Newton down-hill method to speed up the approximation, as outlined in [JM12]. After finding the path, the unbiased result is obtained by the generalized geometry factor in Figure 3.

Manifold Next Event Estimation (MNEE) [HDF15] applies Manifold Exploration to Next Event Estimation (NEE) to connect the path to the light even with the presence of refraction. It is in particular effective to solve the difficult specular-diffuse-specular (SDS) cases. In addition, MNEE improves the equations of Manifold Exploration in Figure 2 by changing the step of finding $\partial x_2$ from $\partial x_4$ to finding $\partial x_2$ from $\partial c_3$.

MNEE can find the caustics caused by refraction but not the caustics caused by reflection. Specular Manifold Sampling (SMS) [ZGJ20] samples all specular objects including reflective surfaces to address the issues with the reflected caustics path. SMS also improves MNEE further by changing the half-vector based constraint function of MNEE to angle-difference based constraint function. The improvement can be clearly seen from Figure 4. In addition

**Algorithm 1:** WalkManifold [JM12]

**Input:** A path $x_1,\ldots,x_n$ before mutation, and a light point $x'_n$.

**Output:** A path $x_2,\ldots,x_{n-1}$ after mutation.

1 Set $i=0$ and $\beta=1$
2 **while** $\|x_n - x'_n\| > \varepsilon L$ **do**
3 $\quad p = x_2 - \beta T(x_2) P_2 A^{-1} B_k T(x_n)^T (x'_n - x_n)$
4 $\quad$ Propagate the ray $x_1 \to p$ through all specular interactions, producing $x_2^+,\ldots,x_n^+$.
5 $\quad$ **if** *step 4 succeeded and* $\|x_n^+ - x'_n\| < \|x_n - x'_n\|$ **then**
6 $\quad\quad x_2,\ldots,x_n = x_2^+,\ldots,x_n^+$
7 $\quad\quad \beta = min(1, 2\beta)$
8 $\quad$ **else**
9 $\quad\quad \beta = \beta/2$
10 $\quad$ **end**
11 $\quad$ Set $i = i+1$, and fail if $i > N$.
12 **end**
13 return $x_2,\ldots,x_{n-1}$

the SMS proposes a two-stage method to work on normal-mapped surfaces, which explores the manifold with surface normal and then explores the manifold with the texture normal.

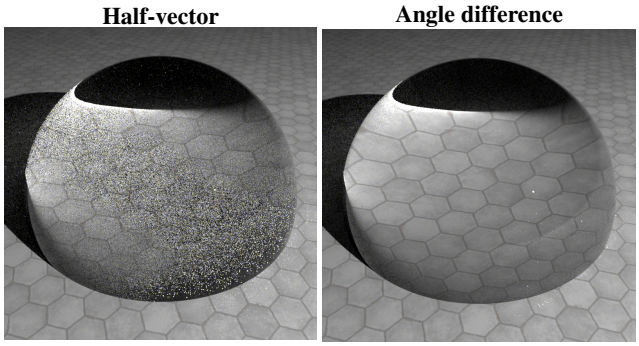


**Figure 4:** *Comparing the constraint function of half-vector (left) and angle difference (right) in 1 spp. Higher manifold walk success rate (SR) means more manifold paths can be found.*

## 4. Specular Manifold Bisection Sampling

We propose Specular Manifold Bisection Sampling (SMBS), an improved version of SMS [ZGJ20]. SMBS is inspired by the small and large mutations in Metropolis Light Transport (MLT) [VG97]. While the Jacobian Matrix of the original SMS method performs well in local convergence (the small mutation), it might fail to find a valid manifold path when the ray deviates too much from the light or bounces from a complex surface. Our proposed SMBS method adds a large mutation step to avoid such a problematic convergence to the local minimum. Figure 5 explains the difference between the small mutation and the large mutation. When any of the specific conditions in Figure 6 occurs, we trigger the large mutation step. Otherwise the small mutation step of the original SMS is followed. The purpose of the large mutation is to find a better search area, which is then followed by the small mutation to approach the correct path. The following subsections further explain our SMBS method in detail.

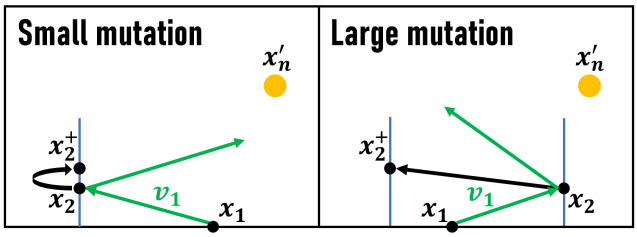


**Figure 5:** *Schematic of the small mutation and the large mutation. The small mutation is the strategy in the original SMS. It explores $x_2^+$ on the adjacent area according to the slope of $x_2$. When $x_2$ is on a back-lit surface, the large mutation is needed to shift $x_2$ to $x_2^+$ and make $v_1$ reflect to $x'_n$.*

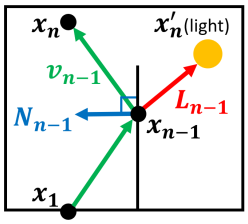


1. Total internal reflection. $refract(v_{k-2}, N_{k-1}, density) = 0$ when $k = 3,\ldots,n$.
2. Backlight. $dot(N_{n-1}, L_{n-1}) < 0$.
3. Large deviation. $dot(v_{n-1}, L_{n-1}) < 0.8$.

**Figure 6:** *Conditions of the large mutation.*

### 4.1. Generating the Initial Path

Regardless of MNEE, SMS, or our SMBS, the initial path must be generated, and then the answer can be slowly approached based on this path. First, trace a ray which starts from the eye. Second, randomly sample a specular surface and a light surface when the ray hits a diffuse surface by random walk. Taking the diffuse surface at $x_1$ as an example, shoot a ray from $x_1$ to the specular surface $x_2$ and get the initial path $x_1,\ldots,x_n$ through multiple refractions and reflections ($x_n$ is non-specular). If the light surface $x'_n$ is not hit in the end, it will use mutation to find the path from $x_1$ to $x'_n$. See 4.2 for a detailed mutation process.

### 4.2. Large Mutation

The path mutation method of SMBS is shown in Algorithm 2. Compared to the previous Algorithm 1, our method adds a condition of large mutation in line 3. We perform a large mutation when the path $x_1,\ldots,x_n$ satisfies one of the conditions described in Figure 6, otherwise we use the small mutation of the original SMS. The first condition occurs at the total internal reflections during a refraction such as the cases in Figure 1. The second condition avoids the back-lit situations where the small mutations usually get stuck. Figure 10 shows an example of such cases. The third condition is designed to avoid too many small mutations which could be costly. Figure 12 offers an example of such cases. Our experiments show

**Algorithm 2:** OurWalkManifold

**Input:** A path $x_1,\ldots,x_n$ before mutation, and a light point $x'_n$.
**Output:** A path $x_2,\ldots,x_{n-1}$ after mutation.

Set $i=0$ and $\beta=1$
**while** $\|x_n-x'_n\|>\varepsilon L$ **do**
  **if** *large mutation (see Figure 6)* **then**
    $v'_2=GetNextDir((x_2,\ldots,x_{n-1}),x'_n)$
    $v_1=normalize(x_2-x_1)$
    $\alpha=GetRatio(x_1,x_2)$
    $\beta=1$
    $p=x_1+(\alpha(-v'_2)+(1-\alpha)v_1)$
  **else**
    $p=x_2-\beta T(x_2)P_2A^{-1}B_kT(x_n)^T(x'_n-x_n)$
  **end**
  Propagate the ray $x_1\rightarrow p$ through all specular interactions, producing $x_2^+,\ldots,x_n^+$.
  **if** *large mutation or step 13 succeeded and* $\|x_n^+-x'_n\|<\|x_n-x'_n\|$ **then**
    $x_2,\ldots,x_n=x_2^+,\ldots,x_n^+$
    $\beta=min(1,2\beta)$
  **else**
    $\beta=\beta/2$
  **end**
  Set $i=i+1$, and fail if $i>N$.
**end**
return $x_2,\ldots,x_{n-1}$

**Algorithm 3:** GetNextDir

**Input:** A path $x_2,\ldots,x_{n-1}$, and a light point $x'_n$.
**Output:** A direction $v'_2$ by large mutation.

$v'_2=normalize(x_{n-1}-x'_n)$
**for** $i=n-1;i>=2;i=i-1$ **do**
  **if** $x_i$ *is a reflective vertex* **then**
    $v'_2=reflect(v'_2,x_i)$
  **else**
    $v'_2=refract(v'_2,x_i)$
  **end**
**end**
return $v'_2$

that a threshold value between 0.8 and 0.9 works well for condition 3.

Ideally, the large mutation quickly finds a better search area and the small mutation approaches the correct path. Therefore, the ideal large mutation must have low complexity and roughly approach the correct path.

Our first thought was to trace back from $x'_n$ to $x_{n-1}$ to get the path $x'_1,\ldots,x'_n$, and then let the next mutation change to shoot a ray from $x_1$ to $x'_2$. But the cost of tracing paths was too high in practice. Instead we use a much simpler approach as shown in Algorithm 3. Let $v'_n$ be a direction of $x'_n$ to $x_{n-1}$. Substitute $v'_n$ and the normal of $x_{n-1}$ into the reflection or refraction formula to get $v'_{n-1}$. Then substitute $v'_{n-1}$ and the normal of $x_{n-2}$ into the reflection or refraction formula to get $v'_{n-2}$. And so on, $-v'_2$ will be the direction of the next mutation.

It is worth mentioning that the stage one of the two-stage SMS [ZGJ20] may be considered a certain kind of large mutation. However, its large mutation is only performed once at the initial stage while our SMBS method may perform large mutation whenever it is necessary (i.e., Algorithm 2, Line 3). Furthermore, while the two-stage SMS works mainly on normal-mapped reflection, our large mutation works on all types of specular surfaces. Figure 12 offers a validation of the above observation.

### 4.3. Interpolation Coefficient $\alpha$

According to Figure 7, in order to make the large mutation more stable, our next sampling direction is the interpolation between the previous direction $v_1$ and the current evaluation direction $-v'_2$. Algorithm 4 shows the formula used to calculate the interpolation coefficient (the offset of the large mutation). Although taking the half-vector of $v_1$ and $-v'_2$ is the easiest method, we have observed that we cannot immediately know whether it is a good mutation toward the direction $-v'_2$. What is a good mutation? That is, the direction can still hit the specular object after the mutation, and the offset on the specular surface should be moderate. Therefore we further check the intersection with the bounding box of the specular object containing $x2$. If the mutation does not hit the specular object, then we reduce the offset toward the direction $-v'_2$.

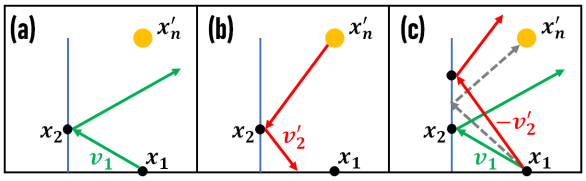


**Figure 7:** *Process of the large mutation. (a) The path before mutation. (b) The path traced backward from the light. (c) The correct path is usually between (a) and (b), so an interpolation of $v_1$ and $-v'_2$ as the direction of mutation is chosen.*

Figure 8 shows that using interpolation coefficient to get the next sampling direction has lower average mutation numbers per path (mpp), which means that a manifold path can be found through fewer mutations. In addition, a good mutation also increases the manifold walk success rate (SR), which means it is easier to find the manifold paths.

### 4.4. Unbiased Results

Finally, we use the same Algorithm 5 as the SMS to get unbiased results. First find a manifold path. Then get the PDF, $p_k$ in Algorithm 5, of the path by randomly sampling manifold paths.

## 5. Results

We modify the open-source version of SMS which is based on Mitsuba2 [Jak20]. Regarding the program, we mainly modified the

**Algorithm 4:** GetRatio

**Input:** The first vertex $x_1$ and the second vertex $x_2$ in the path. The previous direction $v_1$ and the current evaluation direction $-v_2'$.

**Output:** A interpolation coefficient $\alpha$.

$\alpha = 0.5$
**if** $dot(v_1, -v_2') < 0$ **then**
  //backlight such as the right of Figure 5
  $\alpha = 1$
**end**
**while** *true* **do**
  $dir = \alpha(-v_2') + (1-\alpha)v_1$
  **if** $boundingBox(x_2).rayIntersect(x_1, dir).isValid()$ **then**
    break
  **end**
  $\alpha = \alpha * 0.5$
**end**
return $\alpha$

**Algorithm 5:** UnbiasedSMBS

**Input:** The shading point $x_1$ and the light point $x_n$ with density $p(x_n)$.

**Output:** Estimate of radiance traveling from $x_n$ to $x_1$.

$x_2 \leftarrow$ sample a specular vertex
$x_2^* \leftarrow$ the second vertex returned by OurWalkManifold (alg2)
$\langle 1/p_k \rangle = 1$
**while** *true* **do**
  $x_2 \leftarrow$ sample a specular vertex
  $x_2' \leftarrow$ the second vertex returned by OurWalkManifold
  **if** $\|x_2' - x_2^*\| < \varepsilon$ **then**
    break
  **end**
  $\langle 1/p_k \rangle = \langle 1/p_k \rangle + 1$
**end**
return $f_s(x_2^*)G(x_1 \leftrightarrow \ldots \leftrightarrow x_n)\langle 1/p_k \rangle L_e(x_n)/p(x_n)$

content related to the integrator type "path_sms_ms". We run the program on a notebook PC with an Intel® Core™ i7-10875H CPU. The ground truth of each scene is the result of running 1000 samples per pixel (spp) by unbiased SMS. For each comparison, we list the running time, manifold walk success rate (SR), average number of mutations per path (mpp), root mean square error (RMSE) and other information under each algorithm. The higher the success rate (SR), the easier it is for the algorithm to find a manifold path. The lower the mpp, the fewer number of mutations is needed to find a manifold path, which means less computation.

In Figure 9, the area near the refraction surface has a high probability of total internal reflection. When the total internal reflection occurs, SMS will give up on finding a valid path. In contrast, our SMBS can effectively deal with this kind of path with large mutations.

Figure 10 shows an example where back-lit specular surfaces are present. Although it is not a difficult case for the SMS which already has a very high manifold walk success rate, our SMBS can further improve the results because of our large mutation conditions (Figure 6) that detect the back-lit cases.

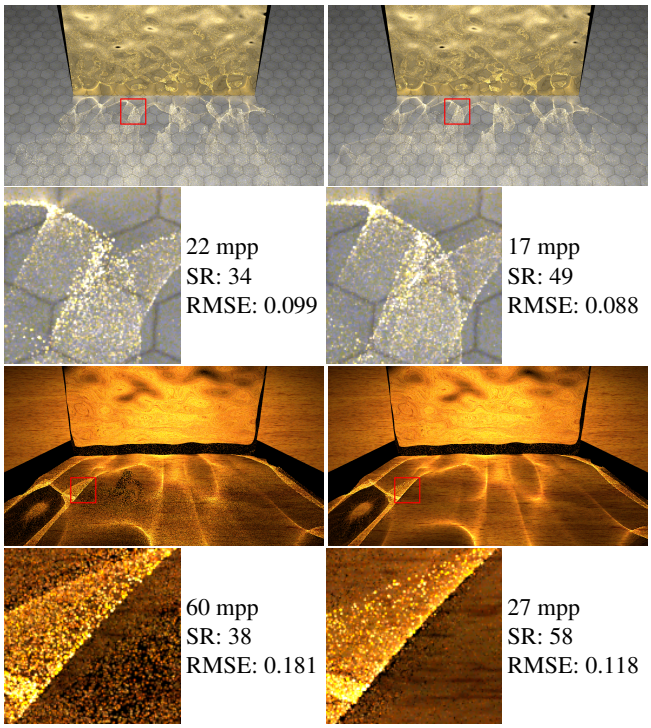


**Figure 8:** *Two scenes showing specular reflective and refractive surfaces, rendered with unbiased SMBS. We show equal-sample comparison (1 spp) between using $-v_2'$ in Figure 7 as the next sampling direction (left) and using interpolation coefficient to get the next sampling direction (right). Insets show average mutation numbers per path (mpp), manifold walk success rate (SR), and root mean square error (RMSE).*

Figure 11 shows that under the equal time, SMS can achieve 2 spp, while SMBS only achieves 1 spp. We find that under the same spp, SMS only need to process about half of the number of rays in SMBS, leading to faster rendering. However the values of success rate show that the number of paths successfully found by SMBS in this scene is about 9 times higher than that of SMS. Therefore, even if SMS has a higher spp in this scene under equal time, our method still has lower RMSE and produces better results.

In the normal-mapped reflection scene of Figure 12, SMBS not only spends less time, but also has lower RMSE. The number of rays of SMBS is about half of SMS because SMBS has lower number of mutations per pixel (mpp). A lower mpp means that SMBS can spend fewer mutations to find a correct manifold path. The success rate of SMBS is also improved because large mutations reduce the probability of local convergence.

We also compare our results to the two-stage SMS [ZGJ20] in Figure 12. As mentioned previously in 4.2, the stage one of the two-stage SMS may be considered a certain kind of large mutation. However, its large mutation is performed once at the initial stage

while our SMBS method may perform large mutation whenever it is necessary. Furthermore, while the two-stage SMS works mainly on normal-mapped reflection, our large mutation works on all types of specular surfaces.

## 6. Conclusions and Future Work

Our SMBS method avoids the problematic convergence to the local minimum in SMS. In scenes with complex reflective or refractive surfaces, our method achieves nearly twice or more improvement when measured in manifold walk success rate (SR) and root mean square error (RMSE).

We have not yet implemented our SMBS method on GPU. How to convert the current method into an algorithm that is more conducive to parallel processing is a possible direction for future work.

The higher manifold walk success rate (SR), the more manifold paths found under the same spp, and the less noise. Therefore, increasing SR helps the convergence of a picture. We think that SR may be further improved by controlling the specular sampling. For example, we may reduce the sampling probability of back-lit specular surfaces because they are less likely to fall on caustics paths.

## 7. Acknowledgment

The work is supported in part by MediaTek Inc. and by the Ministry of Science and Technology (MOST) of Taiwan under grant MOST 110-2221-E-003-015.

## References

[GKDS12] GEORGIEV I., KŘIVÁNEK J., DAVIDOVIČ T., SLUSALLEK P.: Light transport simulation with vertex connection and merging. *ACM Trans. Graph. 31*, 6 (nov 2012). URL: https://doi.org/10.1145/2366145.2366211, doi:10.1145/2366145.2366211. 2

[HDF15] HANIKA J., DROSKE M., FASCIONE L.: Manifold next event estimation. *Comput. Graph. Forum 34*, 4 (jul 2015), 87–97. 2

[Jak20] JAKOB W.: Mitsuba renderer 2, 2020. URL: https://github.com/mitsuba-renderer/mitsuba2. 4

[Jen96] JENSEN H. W.: Global illumination using photon maps. In *Proceedings of the Eurographics Workshop on Rendering Techniques '96* (Berlin, Heidelberg, 1996), Springer-Verlag, p. 21–30. 2

[JM12] JAKOB W., MARSCHNER S.: Manifold exploration: A markov chain monte carlo technique for rendering scenes with difficult specular transport. *ACM Trans. Graph. 31*, 4 (jul 2012). URL: https://doi.org/10.1145/2185520.2185554, doi:10.1145/2185520.2185554. 1, 2, 3

[Kaj86] KAJIYA J. T.: The rendering equation. *SIGGRAPH Comput. Graph. 20*, 4 (aug 1986), 143–150. URL: https://doi.org/10.1145/15886.15902, doi:10.1145/15886.15902. 1, 2

[KSK01] KELEMEN C., SZIRMAY-KALOS L.: *Simple and Robust Mutation Strategy for Metropolis Light Transport Algorithm*. Tech. Rep. TR-186-2-01-18, Institute of Computer Graphics and Algorithms, Vienna University of Technology, Favoritenstrasse 9-11/E193-02, A-1040 Vienna, Austria, jul 2001. human contact: technical-report@cg.tuwien.ac.at. URL: https://www.cg.tuwien.ac.at/research/publications/2001/Szirmay-2001-METR/. 2

[LW93] LAFORTUNE E. P., WILLEMS Y. D.: Bi-directional path tracing. In *PROCEEDINGS OF THIRD INTERNATIONAL CONFERENCE ON COMPUTATIONAL GRAPHICS AND VISUALIZATION TECHNIQUES (COMPUGRAPHICS '93* (1993), pp. 145–153. 2

[SWZ96] SHIRLEY P., WANG C., ZIMMERMAN K.: Monte carlo techniques for direct lighting calculations. *ACM Trans. Graph. 15*, 1 (jan 1996), 1–36. URL: https://doi.org/10.1145/226150.226151, doi:10.1145/226150.226151. 2

[VG97] VEACH E., GUIBAS L. J.: Metropolis light transport. In *Proceedings of the 24th Annual Conference on Computer Graphics and Interactive Techniques* (USA, 1997), SIGGRAPH '97, ACM Press/Addison-Wesley Publishing Co., p. 65–76. URL: https://doi.org/10.1145/258734.258775, doi:10.1145/258734.258775. 1, 2, 3

[Whi80] WHITTED T.: An improved illumination model for shaded display. *Commun. ACM 23*, 6 (jun 1980), 343–349. URL: https://doi.org/10.1145/358876.358882, doi:10.1145/358876.358882. 2

[ZGJ20] ZELTNER T., GEORGIEV I., JAKOB W.: Specular manifold sampling for rendering high-frequency caustics and glints. *ACM Trans. Graph. 39*, 4 (jul 2020). URL: https://doi.org/10.1145/3386569.3392408, doi:10.1145/3386569.3392408. 1, 2, 3, 4, 5

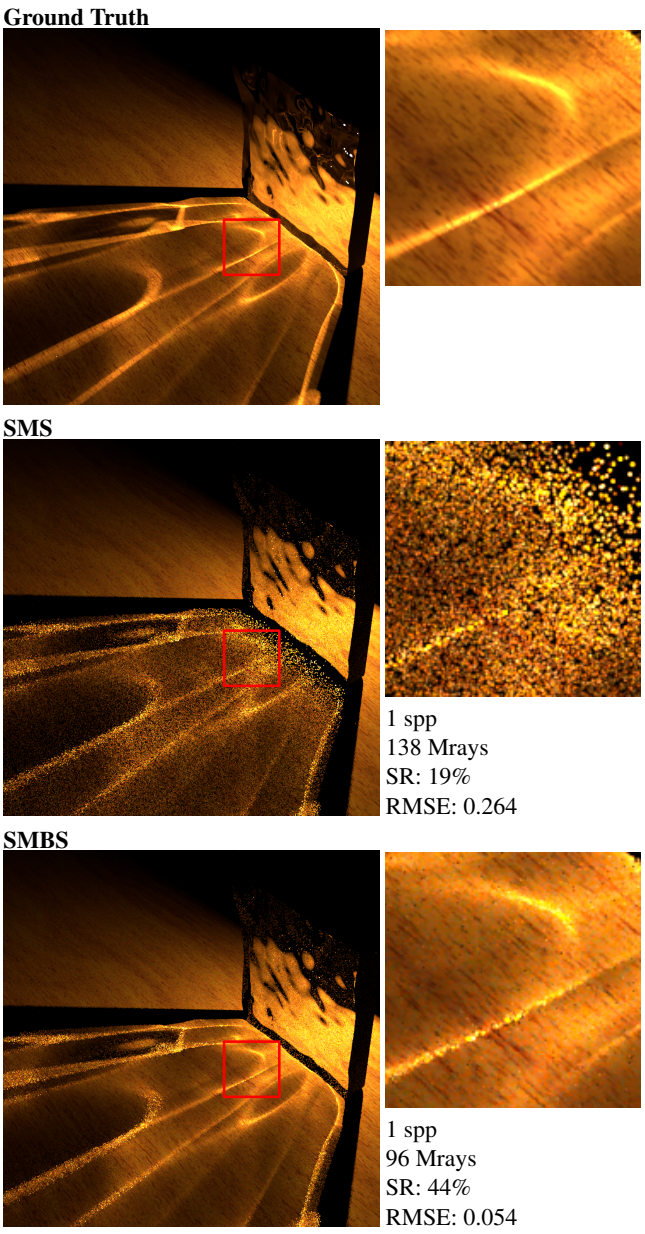


**Figure 9:** *Results of the refraction scenes in roughly equal time (~14 seconds). Insets show samples per pixel (spp), number of rays, manifold walk success rate (SR), and root mean square error (RMSE).*

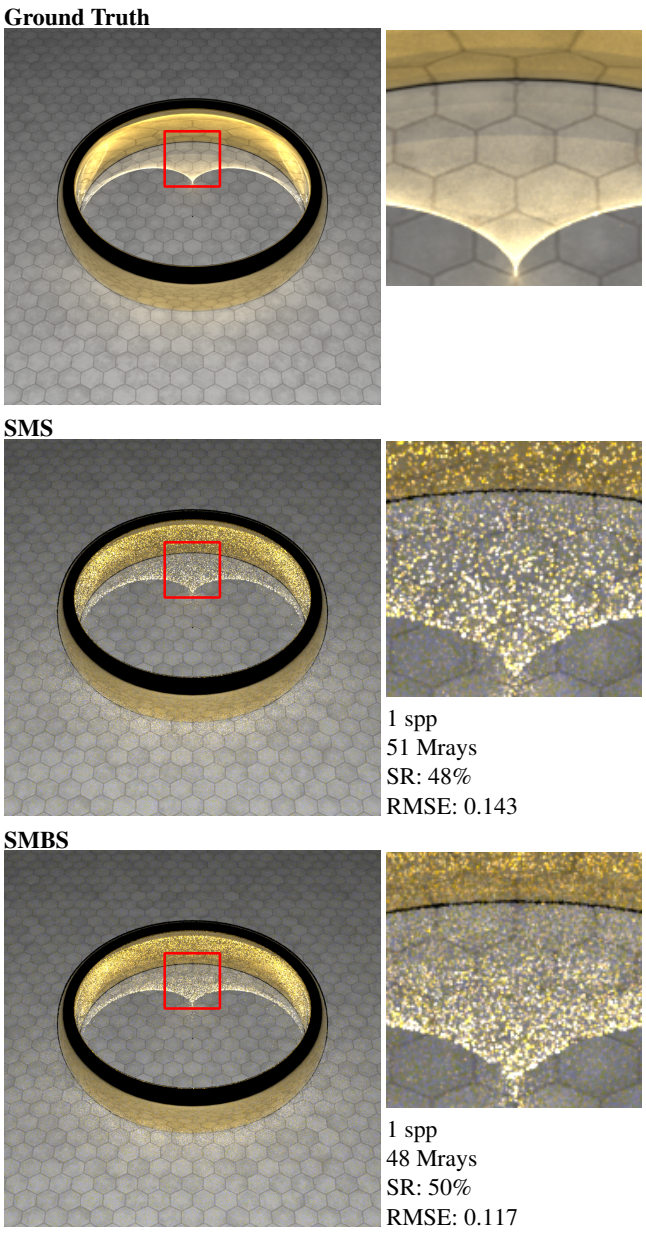


**Figure 10:** *Results of the scenes with backlit area in roughly equal time (~5 seconds). Insets show samples per pixel (spp), number of rays, manifold walk success rate (SR), and root mean square error (RMSE).*

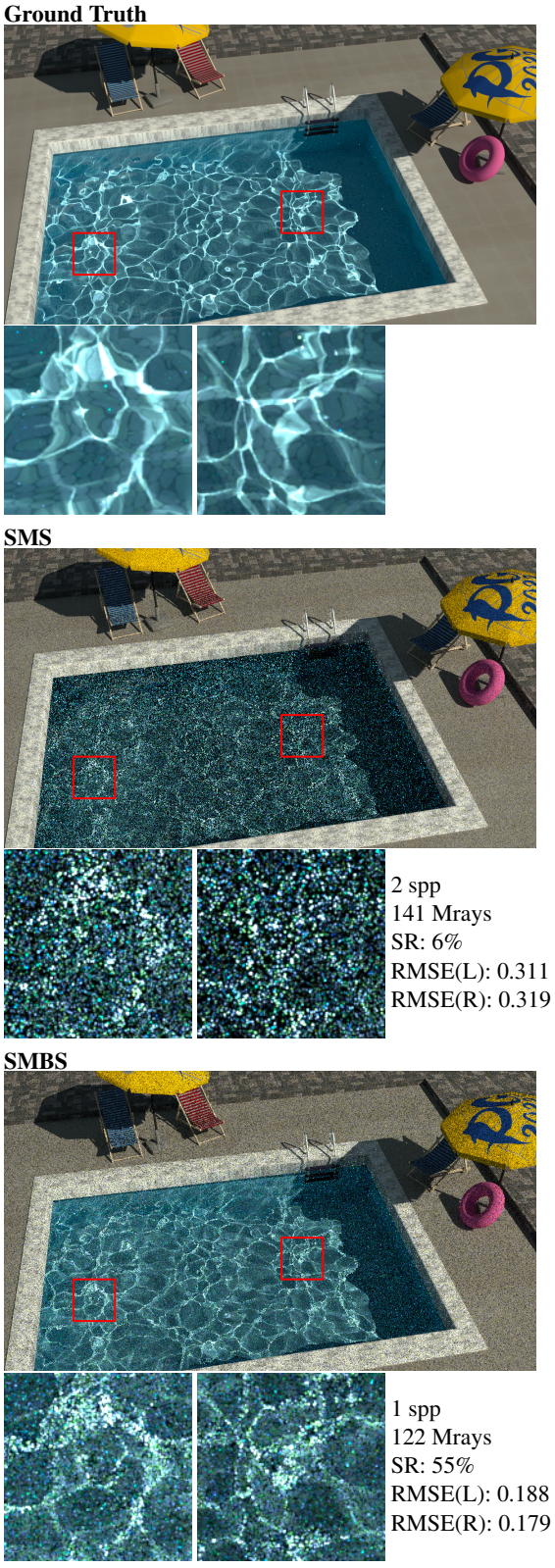


**Figure 11:** *Results of the refraction scenes in roughly equal time (~15 seconds). Insets show samples per pixel (spp), number of rays, manifold walk success rate (SR), and root mean square error (RMSE).*

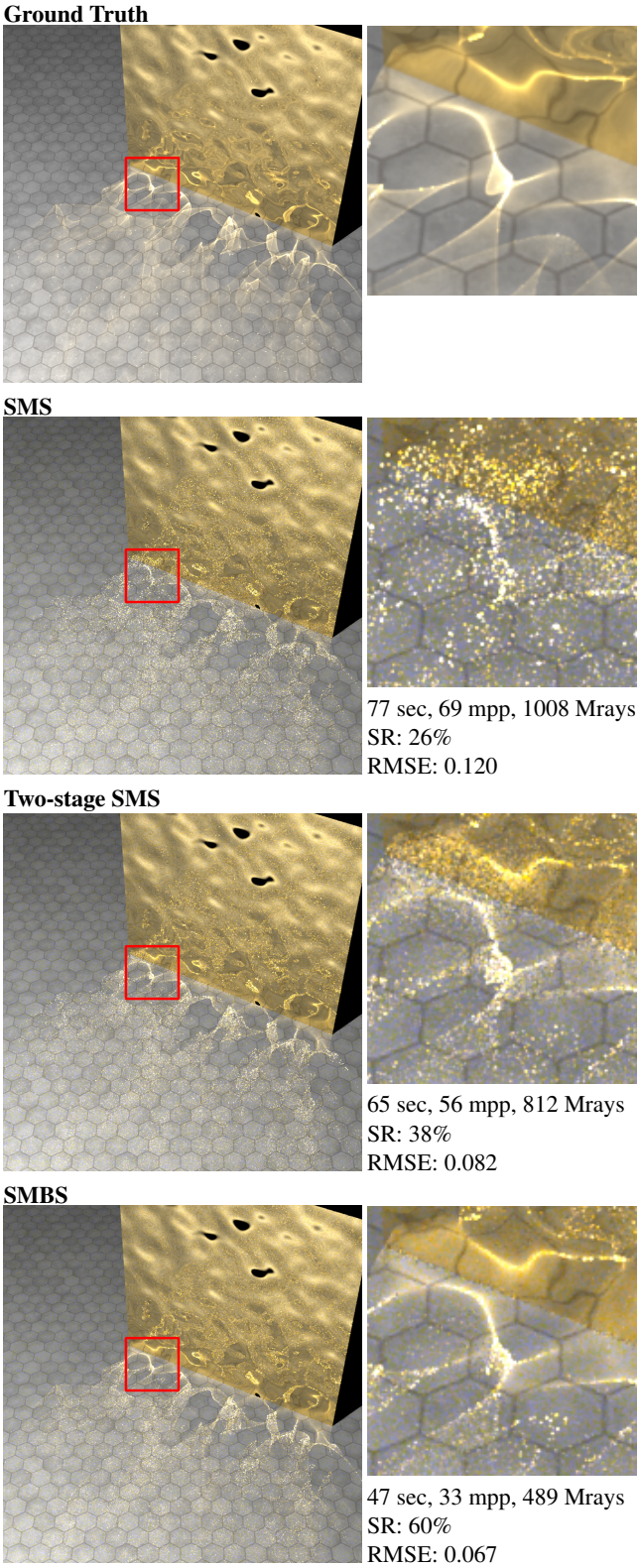


**Figure 12:** *Results of the normal-mapped reflection scene in 1 spp. Insets show running time, average mutation numbers per path (mpp), number of rays, manifold walk success rate (SR), and root mean square error (RMSE).*